

A Hybrid Finite Volume—Finite Element Method for Modeling Flows in Fractured Media

Alexey Chernyshenko, Maxim Olshahskii and Yuri Vassilevski

Abstract This work is devoted to the new hybrid method for solving a coupled system of advection–diffusion equations posed in a bulk domain and on an embedded surface. Systems of this kind arise in many engineering and natural science applications, but we consider the modeling of contaminant transport in fractured porous media as an example of an application. Fractures in a porous medium are considered as sharp interfaces between the surrounding bulk subdomains. The method is based on a monotone nonlinear finite volume scheme for equations posed in the bulk and a trace finite element method for equations posed on the surface. The surface is not fitted by the mesh and can cut through the background mesh in an arbitrary way. The background mesh is an octree grid with cubic cells. The surface intersects an octree grid and we get a polyhedral octree mesh with cut-cells. The numerical properties of the hybrid approach are illustrated in a series of numerical experiments with different embedded geometries. The method demonstrates great flexibility in handling curvilinear or branching embedded structures.

Keywords Finite volume method · TraceFEM · Bulk–surface coupled problems · Fractured porous media · Octree grid

MSC (2010): 65M60 · 65N08 · 65Q60

A. Chernyshenko (✉) · Y. Vassilevski
Institute of Numerical Mathematics, Gubkina 8, Moscow 119333, Russia
e-mail: chernyshenko.a@gmail.com

Y. Vassilevski
e-mail: yuri.vassilevski@gmail.com

M. Olshahskii
Department of Mathematics, University of Houston, Houston, TX 77204-3008, USA
e-mail: molshan@math.uh.edu

1 Introduction

At a recent time, there has been a growing interest in developing methods for the numerical treatment of systems of coupled bulk–surface PDEs. Different approaches can be distinguished depending on how the surface is recovered and equations are treated. If a tetrahedral tessellation of the volume is available that fits the surface, then it is natural to introduce finite element spaces in the volume and on the induced triangulation of the surface. Unfitted finite element methods allow the surface to cut through the background tetrahedral mesh. In the class of finite element methods also known as cutFEM, Nitsche-XFEM or TraceFEM, standard background finite element spaces are employed, while the integration is performed over cut domains and over the embedded surface [2]. The benefits of the unfitted approach are the efficiency in handling implicitly defined surfaces, complex geometries, and the flexibility in dealing with evolving domains. The hybrid method described in this paper belongs to the general class of unfitted methods.

If the finite element method is used for the bulk problem, then it is natural to consider a finite element method for surface PDE as well. However, other discretizations such as finite volume or finite difference methods can be preferred for the PDE posed in the volume.

This paper develops a numerical method based on the sharp-interface representation, which uses a FV-method to discretize the bulk PDE. Our goal is (i) to allow the surface to overlap with the background mesh in an arbitrary way, (ii) to avoid regular triangulating the surface, (iii) to avoid any extension of the surface PDE to the bulk domain. To achieve these goals, we combine the monotone (i.e. satisfying the discrete maximum principle) finite volume method on general meshes [4, 6] with the trace finite element method on octree meshes from [5]. In the octree TraceFEM one considers the bulk finite element space of piecewise trilinear continuous functions and further uses the restrictions (traces) of these functions to the surface. These traces are further used in a variational formulation of the surface PDE. Effectively, this results in the integration of the standard polynomial functions over the (reconstructed) surface. Only degrees of freedom from the cubic cells cut by the surface are active for the surface problem. Surface parametrization is not required, no surface mesh is built, no PDE extension of the surface is needed. The resulting hybrid FV–FE method is very robust with respect to the position of surfaces against the background mesh and is well suited for handling non-smooth surfaces and surfaces given implicitly.

While the present technique can be applied for tetrahedral or more general polyhedral tessellations of the bulk domain, we use octree grid with cubic cells here. The Cartesian structure and built-in hierarchy of octree grids makes mesh adaptation, reconstruction and data access fast and easy. However, an octree grid provides only the first order (staircase) approximation of a general geometry. Allowing the surface to cut through the octree grid in an arbitrary way overcomes this issue, but challenges us with the problem of building efficient bulk–surface discretizations.

We demonstrate that the hybrid TraceFEM–non-linear FV method complements the advantages of using octree grids by delivering the higher order accuracy for both bulk and surface numerical solutions.

2 Mathematical Model

Consider the bulk domain $\Omega \subset \mathbb{R}^3$ and a piecewise smooth surface $\Gamma \subset \Omega$. The surface Γ may have several connected components. If Γ has a boundary, for simplicity we assume that $\partial\Gamma \subset \partial\Omega$, but the model can be extended to immersed surfaces. Thus, we have the subdivision $\overline{\Omega} = \cup_{i=1,\dots,N} \overline{\Omega}_i$ into simply connected subdomains Ω_i such that $\overline{\Omega}_i \cap \overline{\Omega}_j \subset \Gamma$, $i \neq j$.

In each Ω_i , we assume a given Darcy velocity field of the fluid $\mathbf{w}_i(\mathbf{x})$, $\mathbf{x} \in \Omega_i$. By $\mathbf{w}_\Gamma(\mathbf{x})$, $\mathbf{x} \in \Omega_\Gamma$, we denote the velocity field tangential to Γ having the physical meaning of the flow rate through the cross-section of the fracture. Consider an agent that is soluble in the fluid and transported by the flow in the bulk and along the fractures. The fractures are modeled by the surface Γ . The solute volume concentration is denoted by u , $u_i = u|_{\Omega_i}$. The solute surface concentration along Γ is denoted by v . Change of the concentration happens due to convection by the velocity fields \mathbf{w}_i and \mathbf{w}_Γ , diffusive fluxes in Ω_i , diffusive flux on Γ , as well as the fluid exchange and diffusion flux between the fractures and the porous matrix. These coupled processes can be modeled by the following system of equations [1], in subdomains,

$$\begin{cases} \phi_i \frac{\partial u_i}{\partial t} + \operatorname{div}(\mathbf{w}_i u_i - D_i \nabla u_i) = f_i & \text{in } \Omega_i, \\ u_i = v & \text{on } \partial\Omega_i \cap \Gamma, \end{cases} \quad (1)$$

and on the surface,

$$\phi_\Gamma \frac{\partial v}{\partial t} + \operatorname{div}_\Gamma(\mathbf{w}_\Gamma v - d D_\Gamma \nabla_\Gamma v) = F_\Gamma(u) + f_\Gamma \quad \text{on } \Gamma, \quad (2)$$

where we employ the following notations: ∇_Γ , $\operatorname{div}_\Gamma$ denote the surface tangential gradient and divergence operators; $F_\Gamma(u)$ stands for the net flux of the solute per surface area due to fluid leakage and hydrodynamic dispersion; f_i and f_Γ are given source terms in the subdomains and in the fracture; D_i denotes the diffusion tensor in the porous matrix; the surface diffusion tensor is D_Γ . Both D_i , $i = 1, \dots, N$, and D_Γ are symmetric and positive definite; $d > 0$ is the fracture width coefficient; $\phi_i > 0$ and $\phi_\Gamma > 0$ are the constant porosity coefficients for the bulk and the fracture.

The total surface flux $F_\Gamma(u)$ represents the contribution of the bulk to the solute transport in the fracture. The mass balance at Γ leads to the equation

$$F_\Gamma(u) = [-D\mathbf{n} \cdot \nabla u + (\mathbf{n} \cdot \mathbf{w})u]_\Gamma, \quad (3)$$

where \mathbf{n} is a unit normal vector at Γ , $[w(\mathbf{x})]_\Gamma$ denotes the jump of w across Γ in the direction of \mathbf{n} .

If Γ is piecewise smooth, we need additional conditions on the edges, assuming the continuity of concentration, conservation of fluid mass and solute flux. Also we add Dirichlet's boundary conditions for the concentration u and v on $\partial\Omega_D$ and $\partial\Gamma_D$ and homogeneous Neumann's boundary conditions on $\partial\Omega_N$ and $\partial\Gamma_N$, respectively. Initial conditions are given by the known concentration u_0 and v_0 at $t = 0$.

3 Hybrid Finite Volume–Finite Element Method

To produce a grid with an octree hierarchical structure we assume a Cartesian background mesh with cubic cells and allow local refinement of the mesh by sequential division of any cubic cell into 8 cubic subcells. This mesh gives the tessellation \mathcal{T}_h of the computational domain Ω , $\overline{\Omega} = \cup_{T \in \mathcal{T}_h} \overline{T}$. The surface $\Gamma \subset \Omega$ cuts through the mesh in an arbitrary way. For the purpose of numerical integration, instead of Γ we consider Γ_h , a given polygonal approximation of Γ . We assume that similar to Γ , the reconstructed surface Γ_h divides Ω into N subdomains $\Omega_{i,h}$, and $\partial\Gamma_h \subset \partial\Omega$. We do not imply any restrictions on how Γ_h intersects the background mesh. The reconstructed surface Γ_h is a $C^{0,1}$ surface that can be partitioned in planar triangular elements:

$$\Gamma_h = \bigcup_{K \in \mathcal{F}_h} K, \quad (4)$$

where \mathcal{F}_h is the set of all triangular segments K . In practice, we construct Γ_h using Multi-material cubical marching squares algorithm [3].

The induced tessellation of $\Omega_{i,h}$ can be considered as a subdivision of the volume into general polyhedra. Let $\mathcal{T}_{i,h}$ be the tessellation of $\Omega_{i,h}$ into non-intersected polyhedra. For the transport and diffusion in the matrix we apply a non-linear FV method devised on general polyhedral meshes in [4], which is monotone and has compact stencil. The trace of the background mesh on Γ_h induces a ‘triangulation’ of the fracture, which is very irregular, and so we do not use it to build a discretization method. To handle transport and diffusion along the fracture, we first consider finite element space of piecewise trilinear functions for the volume octree mesh \mathcal{T}_h . We further, formally, consider the restrictions (traces) of these background functions on Γ_h and use them in a finite element integral form over Γ_h . Thus the irregular triangulation of Γ_h is used for numerical integration only, while the trial and test functions are tailored to the background regular mesh. It appears that the properties of this trace finite element method are driven by the properties of the background mesh, and they are independent on how Γ_h intersects \mathcal{T}_h . The TraceFEM was devised and first analysed in [7] and extended for the octree meshes in [5]. A natural way to couple two approaches is to use the restriction of the background FE solution on Γ_h as the boundary data for the FV method and to compute the FV two-side fluxes on Γ_h to

4.1 An Example with a Smooth Curved Surface

The first experiment deals with the case when Γ is a smooth surface embedded in a bulk domain Ω . Consider Γ – the unit sphere centered at the origin and $\Omega = [-1, 1]^3$. By Ω_1 we denote the interior of Γ , Ω_2 denotes the exterior part of Ω . Let $\mathbf{v}(\mathbf{x}) = (-y\sqrt{1-z^2}, x\sqrt{1-z^2}, 0)^T$. The transport velocity field is set to be $\mathbf{w}_\Gamma(\mathbf{x}) = \mathbf{v}(\mathbf{x})$ for $\mathbf{x} \in \Gamma$, $\mathbf{w}_i(\mathbf{x}) = \mathbf{v}(\mathbf{x}) + 0.1\mathbf{s}_i$, $\mathbf{s}_1 = (1, 1, 0)^T$, $\mathbf{s}_2 = (2, 1, 0)^T$. Other parameters in (1), (2) are set to be $D_1 = D_2 = I$, $D_\Gamma = 10I$, $I \in \mathbb{R}^{3 \times 3}$ is the identity tensor, $d = 0.1$. In this test we solve for a steady-state solution, so we set $\phi_1 = \phi_2 = \phi_\Gamma = 0$.

For the exact solution on the surface we take $v(\mathbf{x}) = xy \arctan(2z)$ on Γ .

In Ω_2 the bulk concentration u_2 is defined by the same formula as v , and in Ω_1 the bulk concentration is defined by the equality

$$u_1(\mathbf{x}) = xy \arctan(2z) \cdot \exp(1 - |\mathbf{x}|^2) \quad \text{in } \Omega_1.$$

The concentration is continuous across Γ , i.e. the second equation in (1) is satisfied. However, the diffusive flux in (3) is discontinuous across Γ .

We prescribe Dirichlet boundary conditions on $\partial\Omega$. The source terms f_i and f_Γ are computed such that the triple $\{v, u_1, u_2\}$ solves the stationary Eqs. (1)–(2).

Next we apply non-uniform refinement of the bulk mesh, starting with a uniform grid and $h = \frac{1}{4}$. On each refinement step the cells intersected by the surface are refined four times, and the mesh in the bulk is refined one time. The mesh is gradely refined between the surface and bulk cells, see Fig. 1 (right). Table 1 shows the convergence results for the method on the sequence of locally refined grids. The computed solution after one refinement step is demonstrated in Fig. 1. The convergence rates for the fracture solution varies because the refinement is not uniform, but asymptotically the second order can be observed.

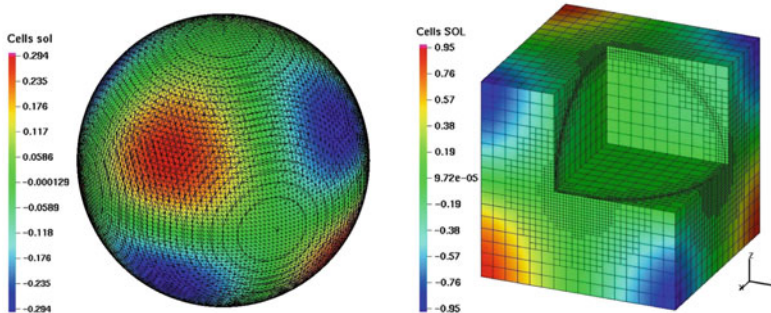


Fig. 1 *Left:* Induced surface mesh and the computed solution on the surface. *Right:* Cutaway of the bulk mesh after one step of local refinement

Table 1 Convergence of numerical solutions in the experiment with a smooth curved Γ and locally refined bulk meshes as in Fig. 1

	#d.o.f.	L^2 -norm	rate	H^1 -norm	rate	L^∞ -norm	rate
3D	120	1.139e-2		1.447e-1		2.817e-2	
	3576	3.457e-3	1.72	5.602e-2	1.37	2.582e-2	0.13
	74176	9.631e-4	1.84	2.111e-2	1.41	7.609e-3	1.76
2D	100	1.043e-2		1.020e-1		1.938e-2	
	1628	1.506e-3	2.79	5.118e-2	0.99	6.467e-3	1.58
	26724	6.134e-4	1.30	2.652e-2	0.95	3.980e-3	0.70

4.2 Steady Analytical Solution for a Triple Fracture Problem

Consider the coupled surface–bulk diffusion problem in the domain $\Omega = [0, 1]^3$ with an embedded piecewise planar Γ . We design Γ to model a branching fracture. In the basic model, $\Gamma = \Gamma(0)$ consists of three planar pieces, $\Gamma(0) = \Gamma_{12} \cup \Gamma_{13} \cup \Gamma_{23}$, $\Gamma_{ij} = \overline{\Omega_i} \cap \overline{\Omega_j}$ $i \neq j$, such that $\Omega_1 = \{\mathbf{x} \in \Omega \mid x < 0.5 \text{ and } y > x\}$, $\Omega_2 = \{\mathbf{x} \in \Omega \mid x > 0.5 \text{ and } y > x - 1\}$, $\Omega_3 = \Omega \setminus (\overline{\Omega_1} \cup \overline{\Omega_2})$.

To model a generic situation when Γ cuts through the background mesh in an arbitrary way, we consider the tessellations of $\Omega = [0, 1]^3$ into three subdomains by a surface $\Gamma(\alpha)$. The surface $\Gamma(\alpha)$ is obtained from $\Gamma(0)$ by applying the clockwise rotation by the angle α around the axis $x = z = 0.5$. We show the results with $\alpha = 20^\circ$. The resulting tessellation of Ω and surfaces mesh are illustrated in Fig. 2.

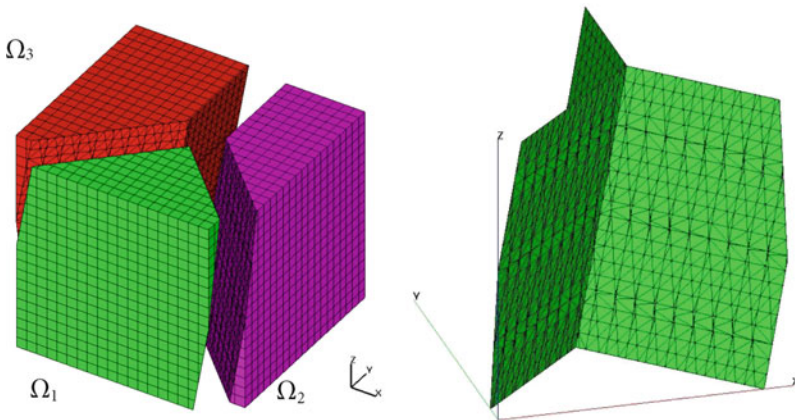


Fig. 2 The figure illustrates the bulk domain with uniform mesh and the surface mesh on the fracture, rotated by 20 degrees

Table 2 The error in the numerical solution for the steady problem with triple fracture, $\alpha = 20$

	#d.o.f.	L^2 -norm	rate	L^∞ -norm	rate
3D	965	6.319e-3		3.754e-2	
	7872	1.805e-3	1.79	1.280e-2	1.55
	63592	5.623e-4	1.80	3.411e-3	1.90
2D	321	7.792e-3		2.716e-2	
	1692	2.084e-3	1.59	5.400e-3	1.94
	7944	7.019e-4	1.41	2.001e-3	1.29

To define the solution $\{v, u\}$ solving the stationary Eq. (1), we introduce

$$\psi_1 = \begin{cases} 16(y - \frac{1}{2})^4, & y > \frac{1}{2} \\ 0, & y \leq \frac{1}{2} \end{cases}, \quad \psi_2 = x - y, \quad \psi_3 = x + y - 1.$$

We define the solution of the basic model problem ($\alpha = 0$)

$$u(\mathbf{x}) = \begin{cases} \sin(2\pi z) \cdot \psi_2(\mathbf{x}) \cdot \phi_3(\mathbf{x}) & \mathbf{x} \in \Omega_1, \\ \sin(2\pi z) \cdot \psi_1(\mathbf{x}) & \mathbf{x} \in \Omega_2, \\ \sin(2\pi z) 2x \cdot \psi_1(\mathbf{x}) & \mathbf{x} \in \Omega_3, \end{cases} \quad v = u|_{\Gamma(0)}.$$

The solution for the problem with rotated fracture is obtained by applying the same rotation. Other parameters are set to be $\mathbf{w} = \mathbf{w}_\Gamma = 0$, $\phi_i = \phi_\Gamma = 0$, $D_i = I$, $D_{\Gamma,i} = 10I$ for $i = 1..3$, and $d_{23} = 0.1$, $d_{13} = d_{12} = \frac{0.1}{\sqrt{2}}$. An interesting feature of this problem is that the surface Γ is only piecewise smooth. The bulk grid is not fitted to the internal edge $\mathcal{E} = \Gamma_{12} \cap \Gamma_{13} \cap \Gamma_{23}$, and hence the tangential derivatives of v are discontinuous inside certain cubic cells from \mathcal{T}_h^Γ . We have the situation, when a kink in v is not resolved in the finite element spaces. This is well-known to result in the $\frac{1}{2}$ -reduction of convergence order. This suboptimal order for a sequence of uniform background meshes is demonstrated by the results in Table 2.

Acknowledgements This work has been supported by RFBF through the grant 16-31-00527 and by NSF through the Division of Mathematical Sciences grant 1522252.

References

1. Alboin, C., Jaffré, J., Roberts, J.E., Serres, C.: Modeling fractures as interfaces for flow and transport. In: Fluid Flow and Transport in Porous Media, Mathematical and Numerical Treatment, vol. 295, p. 13 (2002). American Mathematical Soc
2. Burman, E., Claus, S., Hansbo, P., Larson, M.G., Massing, A.: Cutfem: Discretizing geometry and partial differential equations. Int. J. Numer. Meth. Eng. **104**(7), 472–501 (2015)
3. Chernyshenko, A.: Generation of octree meshes with cut cells in multiple material domains. Num. Methods Progr. **14**, 229–245 (2013). (in russian)

4. Chernyshenko, A., Vassilevski, Y.: A finite volume scheme with the discrete maximum principle for diffusion equations on polyhedral meshes. In: Fuhrmann, J., Ohlberger, M., Rohde, C. (eds.) *Finite Volumes for Complex Applications VII-Methods and Theoretical Aspects*, Springer Proceedings in Mathematics and Statistics, vol. 77, pp. 197–205. Springer International Publishing, Switzerland (2014)
5. Chernyshenko, A.Y., Olshanskii, M.A.: An adaptive octree finite element method for pdes posed on surfaces. *Comput. Methods Appl. Mech. Eng.* **291**, 146–172 (2015)
6. Lipnikov, K., Svyatskiy, D., Vassilevski, Y.: Minimal stencil finite volume scheme with the discrete maximum principle. *Russian J. Numer. Anal. Math. Modelling* **27**(4), 369–385 (2012)
7. Olshanskii, M., Reusken, A., Grande, J.: A finite element method for elliptic equations on surfaces. *SIAM J. Numer. Anal.* **47**, 3339–3358 (2009)